Implementation of Artificial Neural Network (ANN) for Control of CI-SIDO Boost Converter Using DSP

Masters of Technology Phase I
Report

Submitted by

Vinay Pandey

(244102115)

Under the Supervision of

Dr. Shabari Nath

Department of Electronics and Electrical Engineering
Indian Institute of Technology, Guwahati
Jun. 2024

Contents

List of Figures

List of Tables

Abstract

The Coupled Inductor Single-Input Dual-Output (CI-SIDO) boost converter is widely used in modern power electronic systems, including battery-powered and multi-rail power supply applications, where multiple regulated output voltages are required from a single input source. While the converter exhibits a simple voltage conversion relationship in Continuous Conduction Mode (CCM), its behavior in Discontinuous Conduction Mode (DCM) becomes highly nonlinear and depends on load variations and circuit parameters. This creates major challenges for maintaining stable output voltages using conventional analytical or linear control methods.

Previous work in this research implemented an offline Artificial Neural Network (ANN) model to predict the required duty ratio for DCM operation by training the network on simulated data consisting of load voltage, load current, and switching duty. The ANN-based controller eliminated the need for complex mathematical modeling.

The current work extends these contributions by deploying the trained ANN model on a Texas Instruments TMS320F28337D Digital Signal Processor (DSP) for real-time open-loop converter control. The ANN is trained offline in MATLAB and its optimized weights and biases are embedded into C code for DSP execution using Code Composer Studio (CCS). Real-time debugging, variable monitoring, and timing analysis confirm that the DSP executes the feedforward ANN within a single switching cycle, enabling high-frequency operation suitable for power converters. The DSP performs real-time feedforward computations of the neural network by processing input data V_{o1},V_{o2} & I_{o1} and generating corresponding control or prediction outputs D_1 and D_2. The generated pulses are then applied to the CI-SIDO converter switches, allowing the converter to achieve the desired output corresponding to the given reference values.

Chapter 1

Introduction

1.1 Overview

A coupled inductor is used in the power electronics circuit known as the CI-SIDO boost converter to simultaneously increase two output voltages from a single input voltage. When multiple voltage levels are needed, such as in battery charging systems, this configuration is frequently used in power supply designs. Owing to the advantages that SIDO converters provide, ongoing improvements are being made to their topologies in an effort to increase power density, reduce physical dimensions, improve voltage regulation, and increase overall efficiency. Inversely coupled inductor is the type of coupled inductor utilised in the SIDO converter. In inversely coupled inductors, the mutual inductance between the primary and secondary windings is such that the polarity of the induced voltage in the secondary winding opposes the polarity of the primary voltage.

In the CI-SIDO boost converter, during Continuous Conduction Mode (CCM), the input-output voltage relation is similar to that of a normal boost converter and is relatively easy to derive. However, during Discontinuous Conduction Mode , the input-output voltage relation becomes complicated and load-dependent, as well as parameter-dependent. Finding the duty ratio to maintain the output voltage thus becomes more challenging.

Artificial Neural Networks (ANNs) can be used to find the duty ratio when the converter op-

erates in DCM. For an ANN to determine the duty ratio, there is no need for complicated equations. We only need to train it with load voltage, load current and duty ratio data obtained from simulations. Artificial Neural Networks have become one of the most powerful tools for solving complex nonlinear problems such as pattern recognition, system identification, and control applications.

The hardware implementation of an ANN using a DSP enables the trained network to operate in real-time environments where fast decision-making and control actions are critical-such as in power electronics, control of converters. Once the ANN is trained offline in MATLAB, the optimized weights and biases are extracted and transferred to the DSP memory. The DSP performs real-time feedforward computations of the neural network by processing input data and generating corresponding control or prediction outputs.The generated pulses are then applied to the CI-SIDO converter switches, allowing the converter to achieve the desired output corresponding to the given reference values.

Chapter 2

Literature Review

2.1 Single Input Dual Output (SIDO) Converter

In today's fast-paced technological landscape, the use of DC sources has seen a tremendous increase, leading to highly extensive research in DC-DC converters [1]. These research efforts encompass aspects such as reducing size for increased portability, minimizing power loss to enhance efficiency, and streamlining components for cost-effectiveness. In addition to that, many cutting-edge technologies require not just one but multiple levels of voltage sources to operate devices at different voltage levels or charge batteries of varying voltages simultaneously. Isolation devices like flyback converters and forward converters have been developed to transition from a single input to multiple outputs [2]. Additionally, traditional Single Input Single Output converters are used in parallel to provide multiple DC outputs from a single DC source.

However, these design has drawback high device count, high cost, large size and less efficient. Tapping more outputs from a flyback or forward converter poses a challenge due to the interdependence of output voltages. Achieving independent control of the different output voltages becomes difficult [3]. To overcome these challenges, the demand for a DC converter with high efficiency, reduced size, and the capability to supply multiple outputs from a single input has increased. The Single Input Multiple Output (SIMO) converters have become one of the highly demanded research area, because it can convert single DC supply to multiple level DC supply [4]. SIMO converters are far more advantageous than traditional parallel DC-DC converters

due to their smaller size, minimized components, and higher efficiency.

2.2 Coupled Inductor-Single Input Dual Output (CI-SIDO) Converter operation

The CI-SIDO converter has the advantage of producing two regulated DC output voltages from a single unregulated input source. In this study, all components are considered ideal to simplify the analysis. The input voltage source is assumed to have zero internal resistance, and the Inductors and capacitors were treated as ideal elements. The output capacitors are taken to be sufficient to maintain nearly ripple-free output voltages. These assumptions help to understand the basic working and performance of the converter without the effects of real-world losses. Although this idealized model simplifies simulation and analysis, practical results may vary due to the non-ideal behavior of the actual components.

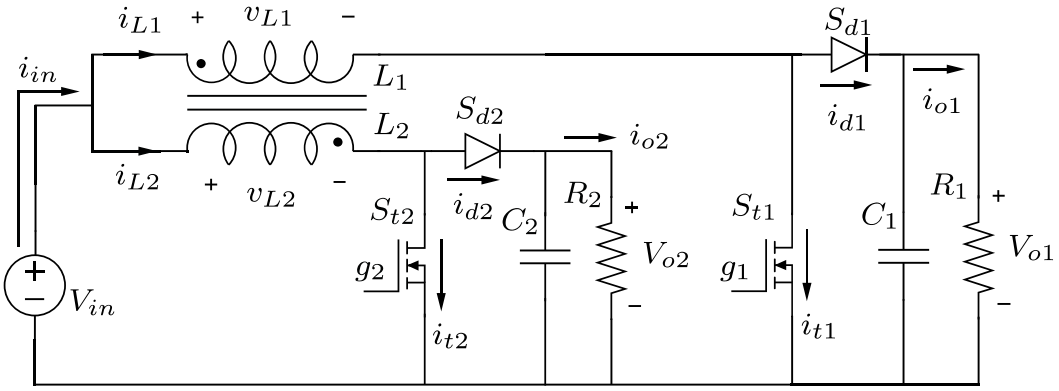

Figure 2.1: CI-SIDO Boost Converter [11]

2.2.1 Distinct Operating Modes in CI-SIDO

The two output voltages of the SIDO boost converter are greater than the shared input voltage. When the MOSFET is switched ON, the diodes become reverse biased, causing energy to be stored in the inductor. On the other hand, when the MOSFET is switched OFF, the energy stored in the inductor is then supplied to the load.

As a result of incorporating two switches (MOSFET - S_{t1}, S_{t2}), SIDO boost converter will have four states. The four states are NN, FF, NF and FF. They are given in Table:2.1,

States	$\boldsymbol{S_{t1}}$	$\boldsymbol{S_{t2}}$
NN	ON	ON
NF	ON	OFF
FN	OFF	ON
FF	OFF	OFF

Table 2.1: Different states of converter

2.2.2 Circuit Equations

The inductor voltages v_{L1} and v_{L2}, capacitor currents i_{C1} and i_{C2} can be calculated for all four states. The following equation are given by [11],

For state NN,

$$\begin{aligned} v_{L1} &= V_{in} \\ i_{C1} &= -\frac{V_{o1}}{R_1} \\ v_{L2} &= V_{in} \\ i_{C2} &= -\frac{V_{o2}}{R_2} \end{aligned} \tag{2.1}$$

For state NF,

$$\begin{aligned} v_{L1} &= V_{in} \\ i_{C1} &= -\frac{V_{o1}}{R_1} \\ v_{L2} &= V_{in} - V_{o2} \\ i_{C2} &= I_{L2} - \frac{V_{o2}}{R_2} \end{aligned} \tag{2.2}$$

For state FN,

$$\begin{aligned} v_{L1} &= V_{in} - V_{o1} \\ i_{C1} &= I_{L1} - \frac{V_{o1}}{R_1} \\ v_{L2} &= V_{in} \\ i_{C2} &= \frac{V_{o2}}{R_2} \end{aligned} \tag{2.3}$$

For state FF,

$$\begin{aligned} v_{L1} &= V_{in} - V_{o1} \\ i_{C1} &= I_{L1} - \frac{V_{o1}}{R_1} \\ v_{L2} &= V_{in} - V_{o2} \\ i_{C2} &= I_{L2} - \frac{V_{o2}}{R_2} \end{aligned} \tag{2.4}$$

Where,

v_{L1} = Instantaneous voltage across inductor L_1

v_{L2} = Instantaneous voltage across inductor L_2

I_{L1} = Average current of inductor L_1

I_{L2} = Average current of inductor L_2

i_{c1} = Instantaneous current of capacitor C_1

i_{c2} = Instantaneous current of capacitor C_2

V_{in} = Average input voltage

V_{o1} = Average output voltage across resistor R_1

V_{o2} = Average output voltage across resistor R_2

By applying volt-sec balance in v_{L1} and v_{L1} using (2.1, 2.2, 2.3, 2.4), input and output relation of SIDO converter is obtained in Continuous Conduction Mode (CCM) mode [11].

$$\begin{aligned} V_{o1} &= \frac{V_{in}}{(1 - D_1)} \\ V_{o2} &= \frac{V_{in}}{(1 - D_2)} \end{aligned} \tag{2.5}$$

By applying KVL, in Fig. 2.1 instantaneous inductor voltages is obtained. Where M is the mutual inductance, $M = \sqrt{L1L2}$. The following equation(2.6) is given by [11].

$$\begin{aligned} v_{L1} &= L_1 \frac{di_{L1}}{dt} - M \frac{di_{L2}}{dt}, \\ v_{L2} &= L_2 \frac{di_{L2}}{dt} - M \frac{di_{L1}}{dt} \end{aligned} \tag{2.6}$$

Similar like Continuous Conduction Mode, four parameters $rd_{NF1}, rd_{NF2}, rd_{FN1}$ & rd_{FN2} are

derived from coupled inductors and mutual inductance between them [11]. But, here instead of duty ratios, voltage ratio between input voltage and output voltage of the converter is used to group sectors. And a total of 9 sectors is obtained.

$$
\begin{aligned}
rd_{FN1} &= \frac{1}{(1+k\sqrt{\frac{L_1}{L_2}})} \\
rd_{FN2} &= \frac{k\sqrt{\frac{L_2}{L_1}}}{(1+k\sqrt{\frac{L_2}{L_1}})} \\
rd_{NF1} &= \frac{k\sqrt{\frac{L_1}{L_2}}}{(1+k\sqrt{\frac{L_1}{L_2}})} \\
rd_{NF2} &= \frac{1}{(1+k\sqrt{\frac{L_2}{L_1}})}
\end{aligned}
\tag{2.7}
$$

It is observed that $rd_{NF1} < rd_{NF2}$ and $rd_{FN2} < rd_{FN1}$. If we plot these values in $\frac{V_{in}}{V_{o1}}$ versus $\frac{V_{in}}{V_{o2}}$ we can obtain 9 sectors as shown in Fig (2.2). The body diode (S_{DB1}) of the MOSFET of the first converter turns on in sector 1, 2 and 3 only. The inductor current pattern varies for all different 9 sectors.

where,

G_{NF1} = Slope of I_{L1} during NF state.

G_{NF2} = Slope of I_{L2} during NF state.

G_{FN1} = Slope of I_{L1} during FN state.

G_{FN2} = Slope of I_{L2} during FN state.

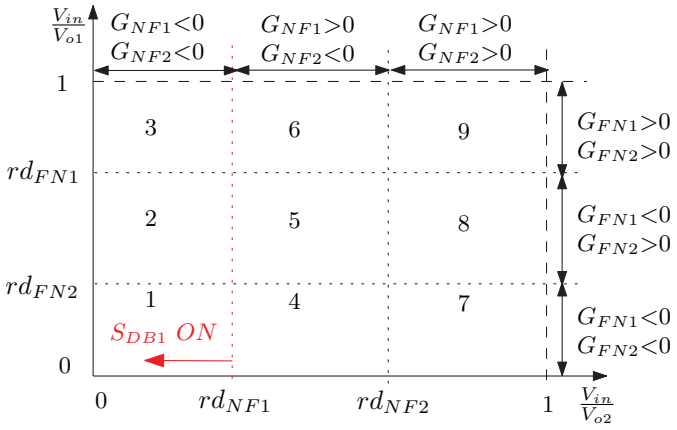

Figure 2.2: Sectors of CI-SIDO Boost Converter in DCM [11]

2.3 Analysis of All Sectors and Operating Modes of the CI-SIDO Boost Converter with One Converter in DCM and the Other in CCM

This chapter presents the waveforms corresponding to all the sectors and modes of the CI-SIDO boost converter. The durations of various states for each sector and mode are also derived. All the figures and equations are adapted from [11].

2.3.1 Sector 1 and 2

Modes 1a and 2a

The waveforms of Mode 1a is shown in Fig. 2.3a and Mode 2a is shown in Fig. 2.3b. Using the figure, the analysis is presented below:

The following equation (2.8 & 2.9) is given by [11]. The obtained values of $i_{o1} = i_{o1bd}$, and $D_1 = t_{NN}$ at the CCM/DCM boundary are–

$$i_{o1bd} = \frac{T_s}{2}[t_{NN}|G_{NN1}|(D_2 - t_{NN}) + (1 - D_2)(1 - t_{NN})|G_{FF1}|], \tag{2.8}$$

where,

$$t_{NN} = \frac{D_2|G_{FN1}| + (1 - D_2)|G_{FF1}|}{G_{NN1} + G_{FN1}} \tag{2.9}$$

Therefore, to operate the converter in Sector 2, $i_{o1b} < i_{o1} < i_{o1bd}$ and $D_{1b} < D_1 < t_{NN}$.

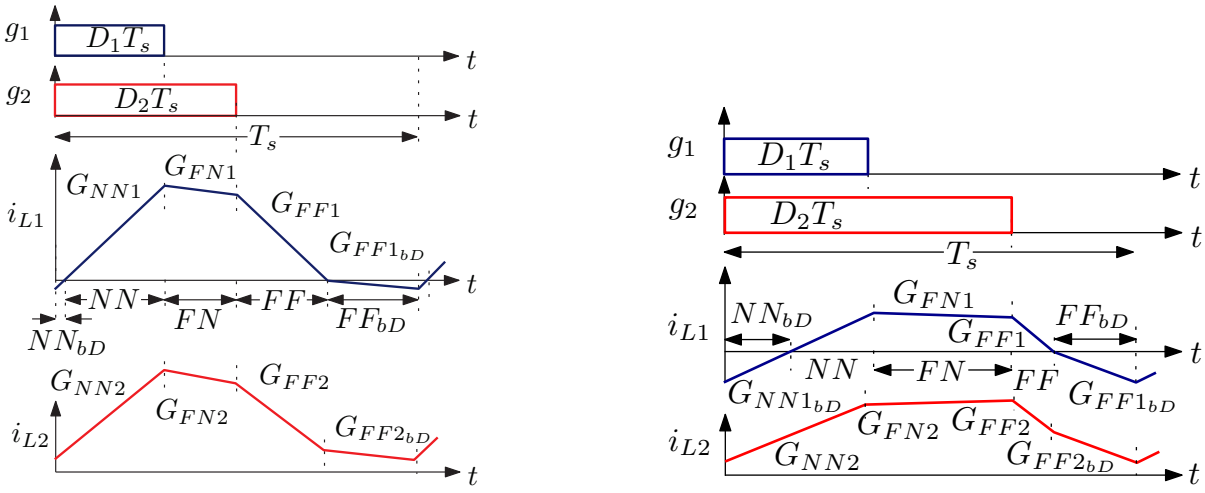

(a) Mode 1a

(b) Mode 2a

Figure 2.3: Theoretical waveforms of g_1, g_2, i_{L1}, i_{L2} during the operation of CI-SIDO boost converter in Mode 1a and 2a converter.[11]

Modes 1b and 2b

The waveforms of Mode 1b and Mode 2b is shown in Fig. 2.4a and Fig. 2.4b respectively.The following equation (2.10 & 2.11) is given by [11].

Finding the values of $i_{o1} = i_{o1\_1b}$ and $D_1 = D_{1\_1b}$ at Mode 1b, we obtain–

$$i_{o1\_1b} = \frac{|G_{FN1}| * (D_2 T_s G_{NN1} - |G_{FN1}|(1-D_2)T_s)^2}{2T_s(|G_{FN1}| + G_{NN1})^2} \tag{2.10}$$

$$D_{1\_1b} = \frac{D_2 G_{FN1} + (1-D_2) G_{NF1}}{G_{NN1} + G_{FN1}} \tag{2.11}$$

At $i_{o1} = i_{o1\_1b}$ and $D_1 = D_{1\_1b}$, the CI-SIDO converter is at Mode 1b. After that, if $D_1 < D_{1\_1b}$ and$i_{o1} < i_{o1_1b}$, this converter operates in Mode 1c.

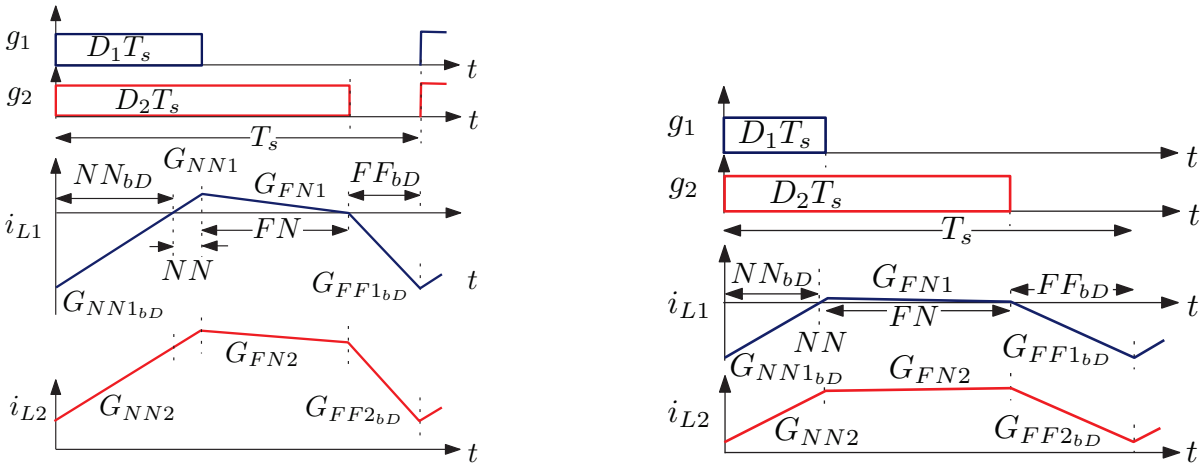

(a) Mode 1b

(b) Mode 2b

Figure 2.4: Theoretical waveforms of g_1, g_2, i_{L1}, i_{L2} during the operation of CI-SIDO boost converter in Mode 1b and Mode 2b converter.[11]

Modes 1c and 2c

The waveforms of Mode 1c is shown in Fig. 2.5a and Mode 2c in Fig. 2.5b.

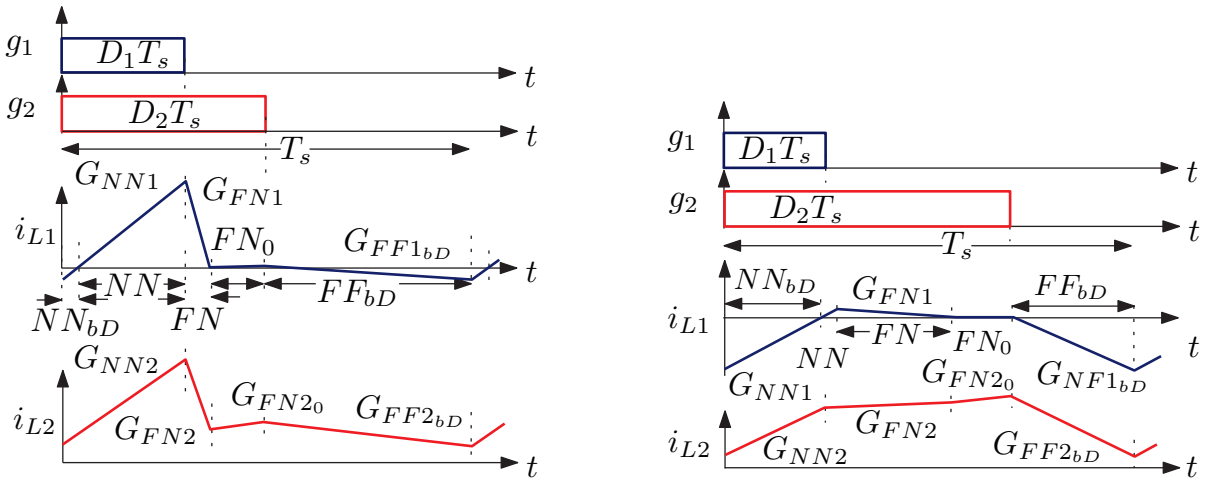

(a) Mode 1c

(b) Mode 2c

Figure 2.5: Theoretical waveforms of g_1, g_2, i_{L1}, i_{L2} during the operation of CI-SIDO boost converter in Mode 1c and 2c converter.[11]

2.3.2 Sector 3

The waveform of the CI-SIDO boost converter operating in Sector–3 is shown in Fig. 2.6. The corresponding time durations for each interval are derived and explained as follows:

The following equation (2.12 & 2.13) is given by [11]. The boundary values of load currents and duty ratios are–

where,

$$t_{NN} = \frac{(1-D_2)|G_{FF1}| - D_2 G_{FN1}}{(G_{NN1} - G_{FN1})}. \tag{2.12}$$

$$D_{1bd} = t_{NN}.$$

Therefore, to operate the converter in Sector 3, $i_{o1} < i_{o1bd}$ and $D_1 < D_{1bd}$.

$$i_{o1_bd} = \frac{T_s}{2}[t_{NN}(D_2 - t_{NN})G_{NN1} + (1-D_2)t_{NN}|G_{FF1}|] \tag{2.13}$$

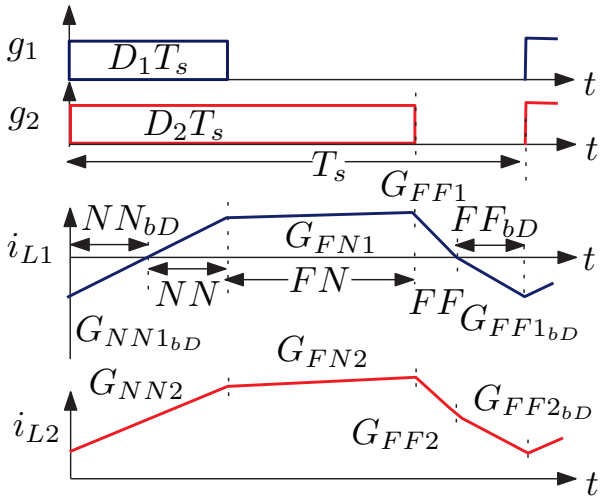

Figure 2.6: Theoretical waveforms of g_1, g_2, i_{L1}, i_{L2} during the operation of CI-SIDO boost converter in sector 3 of converter.[11]

2.3.3 Sectors 4, 5, 7, 8

Modes 4a, 5a, 7a, and 8a

The waveforms of Modes 4a, 5a, 7a and 8a are shown in Figs. 2.7, and The following equation (2.14 , 2.15 & 2.16) is given by [11].

At CCM/DCM boundary, $t_{FF} = (1 - D_2)$, the boundary values of load current and duty ratios are given by–

$$i_{o1bd} = \frac{T_s}{2}\left[t_{NN}G_{NN1}(D_2 - t_{NN}) + (1 - D_2)(1 - t_{NN})|G_{FF1}|\right] \tag{2.14}$$

where,

$$t_{NN} = \frac{|G_{FN1}|D_2 + |G_{FF1}|(1 - D_2)}{G_{NN1} + G_{FN1}} \tag{2.15}$$

$$D_1 = t_{NN}. \tag{2.16}$$

Therefore, i_{L1} remains in Mode 4a when $i_{o1_{4b}} < i_{o1} < i_{o1bd}$ and $D_{1_{4b}} < D_1 < t_{NN}$.

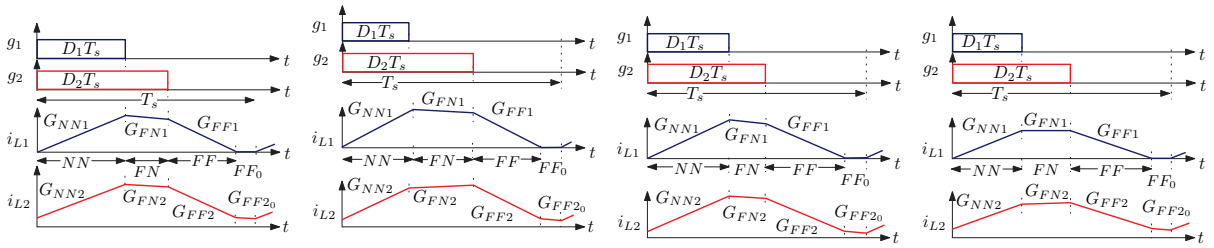

(a) Mode 4a (b) Mode 5a (c) Mode 7a (d) Mode 8a

Figure 2.7: The theoretical waveforms of g_1, g_2, i_{L1}, and i_{L2} corresponding to the operation of the CI-SIDO boost converter in Modes 4a, 5a, 7a, and 8a.[11]

Modes 4b, 5b, 7b and 8b

The waveforms of Modes 4b, 5b, 7b and 8b are shown in Figs. respectively. and The following equation(2.17) & fig. (2.8) is given by [11].

Finding the values of $i_{o1} = i_{o14b}$ and $D_1 = D_{14b}$ for sector 4b, we obtain–

$$i_{o14b} = \frac{|G_{FN1}|G_{NN1}^2 D_2^2 T_s}{2(G_{NN1} + |G_{FN1}|)^2}, \qquad D_{14b} = \frac{D_2 G_{FN1}}{G_{NN1} + G_{FN1}} \tag{2.17}$$

At $i_{o1} = i_{o14b}$ and $D_1 = D_{14b}$, the converter is at Mode 4b. After that, if $i_{o1} < i_{o14b}$ and $D_1 < D_{14b}$, the converter operates in Mode 4c.

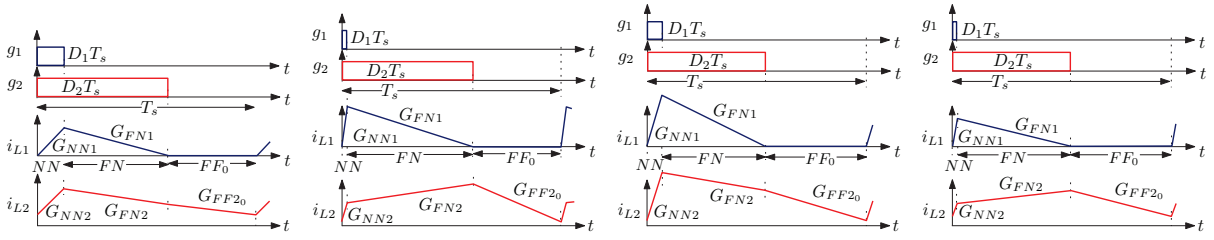

(a) Mode 4b (b) Mode 5b (c) Mode 7b (d) Mode 8b

Figure 2.8: The theoretical waveforms of g_1, g_2, i_{L1}, and i_{L2} corresponding to the operation of the CI-SIDO boost converter in Modes 4b, 5b, 7b, and 8b.[11]

Modes 4c, 5c, 7c and 8c

The waveforms of Modes 4c, 5c, 7c and 8c are shown in Figs. 2.9a, 2.9b, 2.9c and 2.9d respectively.

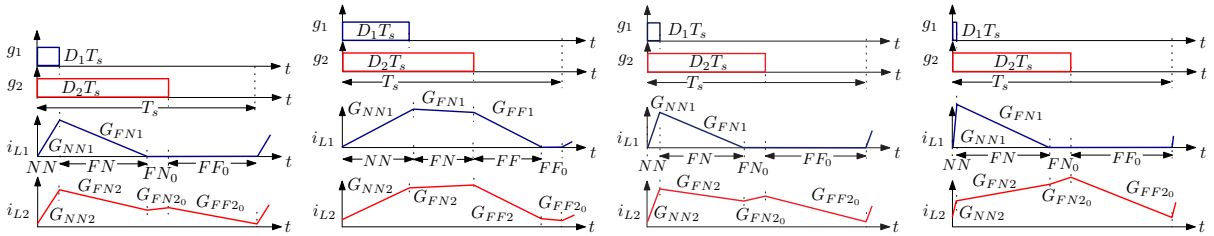

(a) Mode 4c (b) Mode 5c (c) Mode 7c (d) Mode 8c

Figure 2.9: The theoretical waveforms of g_1, g_2, i_{L1}, and i_{L2} corresponding to the operation of the CI-SIDO boost converter in Modes 4c, 5c, 7c, and 8c.[11]

2.3.4 Sector 6 and 9

The waveforms of these Modes 6 and 9 are shown in Figs. 2.9a and 2.9b respectively. and The following equation(2.18 & 2.19) and fig. (2.10) is given by [11].

At CCM/DCM boundary, $t_{FF} = (1 - D_2)$. the boundary values of load current and duty ratios are given by–

$$i_{o1bd} = \frac{T_s}{2}\left[t_{NN}(D_2 - t_{NN})G_{NN1} + (1 - D_2)(1 - t_{NN})|G_{FF1}|\right], \tag{2.18}$$

$$t_{NN} = \frac{(1 - D_2)|G_{FF1}| - D_2 G_{FN1}}{(G_{NN1} - G_{FN1})}. \tag{2.19}$$

Therefore, to operate the converter in Sector 6 and 9, $i_{o1} < i_{o1bd}$ and $D_1 < D_{1bd}$.

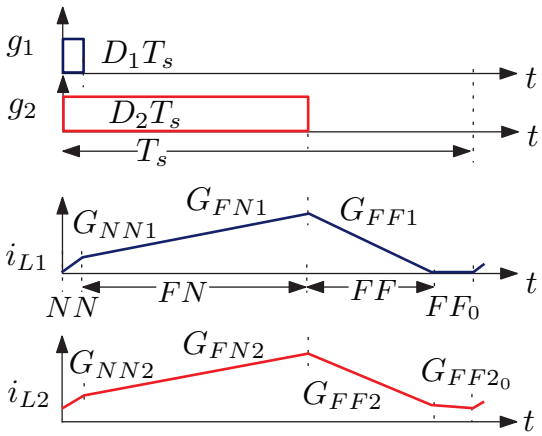

(a) Mode 6

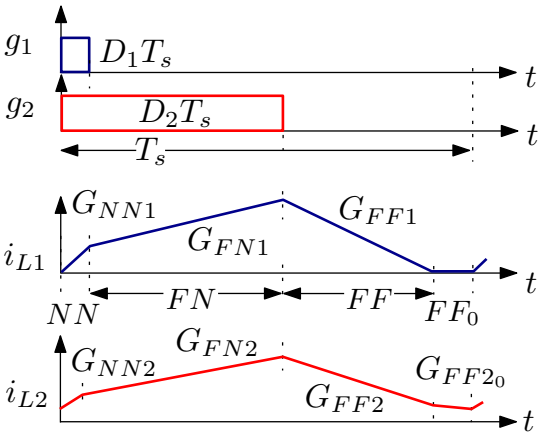

(b) Mode 9

Figure 2.10: The theoretical waveforms of g_1, g_2, i_{L1}, and i_{L2}, when operating in Sector 6 & 9 of CI-SIDO boost converter.[11]

Chapter 3

Artificial Neural Network (ANN)

When the CI-SIDO boost converter operates in the CCM mode, input output relation can be derived easily, which is simply $V_{out} = \frac{V_{in}}{(1-D)}$. But during DCM operation accurately modelling input output relation of the CI-SIDO converter will be challenging. Due to non-linearity and parameter sensitivity.

3.1 Feed-Forward and Back-Propagation Algorithm

It consists of two main phases: the forward Propagation and the backward Propagation. The algorithm adjusts the weights of the network to minimize the difference between the actual output and the desired output.

3.1.1 Forward Propagation

The forward Propagation involves propagating the input data through the network to obtain the output.

1. **Input Layer:** The input data is fed into the input layer of the network. Number of neurons in the output layer depends on the number of inputs to the ANN.
2. **Hidden Layers:** Each neuron in a hidden layer computes its output using an activation

function applied to the weighted sum of its inputs.

3. **Output Layer:** The final output is generated by the neurons in the output layer, where the number of neurons corresponds to the number of outputs required from the ANN.

$$v_j^{[l]}(n) = \sum_{i=0}^{m} w_{ji}^{[l]}(n)\ y_j^{[l-1]}(n) \tag{3.1}$$

Where,

$\boldsymbol{j}$ is the index of neuron at present layer,

$\boldsymbol{i}$ is the index of neuron at previous layer,

$\boldsymbol{(n)}$ represents the n_{th} pattern while training the ANN,

$\boldsymbol{y_i^{[l-1]}(n)}$ is the activation value from previous layer,

$\boldsymbol{w_{ji}^{[l]}(n)}$ is the weights between layer $[l-1]$ and layer $[l]$,

$\boldsymbol{v_j^{[l]}}$ is the net input to the j^{th} neuron,

$\boldsymbol{l}$ is the index of layers $l \in (1, L)$ (L= total number of layers).

$$y_i^{[l]}(n) = \phi(v_j^{[l]}(n)) \tag{3.2}$$

Where,

$\boldsymbol{\phi}$ is the activation function,

$\boldsymbol{y_i^{[l]}(n)}$ is the activation value from present layer.

3.1.2 Backward Propagation

The backward propagation, adjusts the weights and biases of the network to minimize the error between the predicted output and the actual target.To update the weight matrix, we need to find the derivative of the error function with respect to the weights of the ANN. The update $\boldsymbol{\Delta w_{ji}}$

$$\Delta w_{ji}^{[l]}(n) = \frac{\delta E(n)}{\delta w_{ji}(n)} \tag{3.3}$$

The direct derivative of this is complicated, so it is calculated using the chain rule for simplification.[15]

$$\frac{\delta E(n)}{\delta w_{ji}(n)} = \frac{\delta E(n)}{\delta e_j(n)} \cdot \frac{\delta e_j(n)}{\delta y_j(n)} \cdot \frac{\delta y_j(n)}{\delta v_j(n)} \cdot \frac{\delta v_j(n)}{\delta w_{ji}(n)} \tag{3.4}$$

By solving,

$$\frac{\delta E(n)}{\delta e_j(n)} = e_j(n) \qquad \frac{\delta e_j(n)}{\delta y_j(n)} = -1$$

$$\frac{\delta y_j(n)}{\delta v_j(n)} = \phi'(v_j(n)) \qquad \frac{\delta v_j(n)}{\delta w_{ji}(n)} = y_i(n)$$

Where,

$\boldsymbol{E(n)}$ is error function, $\boldsymbol{e_j(n)}$ instantaneous error of the j^{th} neuron,

$\boldsymbol{y_j(n)}$ is output of the j^{th} neuron, $\boldsymbol{v_j(n)}$ is activation value to the j^{th} neuron,

$\boldsymbol{\phi'(.)}$ is derivative of activation function of the j^{th} neuron,

$\boldsymbol{w_{ji}(n)}$ is weight between the neuron j and neuron i.

Therefore the equation 3.4 becomes,

$$\Delta w_{ji}(n) = -\eta\, \delta_j(n)\, y_i(n) \tag{3.5}$$

1. **Calculate Local Gradient $\boldsymbol{\delta_p(n)}$:** Local gradient is the derivative of error function with respect to the activation input to the neuron. For each we have to calculate local gradient. Let $\boldsymbol{p}$ is the index of neuron at the output layer, for output layer the local gradient can be easily calculated as,

$$\delta_p^{[L]}(n) = \frac{\delta E(n)}{\delta v_p^{[L]}(n)} \tag{3.6}$$

   Where, $\boldsymbol{E(n)}$ is the Mean Squared Error function, given by

$$E(n) = \frac{1}{m_L} \sum_{p \in m_L} e_p^{[L]^2}(n) \tag{3.7}$$

$$e_p^{[L]}(n) = y_p^{[L]}(n) - d_p(n) \tag{3.8}$$

   $\boldsymbol{m_L}$ total number of neurons in the output layer,

   $\boldsymbol{e_p^{[L]}(n)}$ is the instantaneous error in the output layer of the p^{th} neuron,

   $\boldsymbol{d_p(n)}$ is the desired output value from the p^{th} neuron,

   $\boldsymbol{y_p^{[L]}(n)}$ is the obtained value from the p^{th} neuron,

   $\boldsymbol{v_p^{[L]}(n)}$ is net activation input to the p_{th} neuron.

2. **Propagate Error Backward:** Now for each hidden layer we have to calculate local gradient. Let j be a index of neuron in a hidden layer and k be a index of neuron of next

layer. The local gradient $\delta_j^{[l]}(n)$ can be calculated by,[15]

$$\delta_j^{[l]}(n) = \frac{\delta E(n)}{\delta v_j^{[l]}(n)} \tag{3.9}$$

$\delta E(n)$ belongs to the output layer and $\delta v_j^{[l]}(n)$ belongs to the different layer. This derivation cannot be obtained directly. So, we need to use chain rule of derivative and the generalized form is,[15]

$$\delta_j^{[l]}(n) = (\sum \delta_k^{[l+1]}(n)\ w_{kj}^{[l+1]}(n))\ \phi'(v_j^{[l]}(n)) \tag{3.10}$$

Where,
$\boldsymbol{\delta_j^{[l]}(n)}$ is local gradient of j_{th} neuron of the layer $[l]$,
$\boldsymbol{\delta_k^{[l+1]}(n)}$ is local gradient of k_{th} neuron of the next layer $[l+1]$,
$\boldsymbol{w_{kj}^{[l+1]}(n)}$ is weights between layer $([l])$ and the layer $([l+1])$.

3. **Update Weights:** Adjust the weights and biases using the computed local gradient. [15]

$$\Delta w_{kj}^{[l]}(n) = -\eta\ \delta_k^{[l]}(n)\ y_j^{[l-1]}(n) \tag{3.11}$$

Where, $l \in (1, L)$ is the index of layers.

$$w_{kj}^{[l]}(n)^{new} = w_{kj}^{[l]}(n)^{old} - \eta\ \delta_k^{[l]}(n)\ y_j^{[l-1]}(n) \tag{3.12}$$

Therefore the weight matrix of all the layer can be updated.

Chapter 4

Implementation of ANN as CI-SIDO Converter Controller

Designing the ANN architecture and training the ANN play crucial roles in implementing the ANN as a controller for the CI-SIDO converter. In this context, the load voltage and load current of the first converter will serve as inputs to the ANN, while the duty ratio for the first converter will be the output from the ANN. This duty ratio will be applied to the converter to obtain the desired output voltage. This chapter focuses on explaining the architecture of the ANN and the process of collecting data to train the ANN model.

4.0.1 Running Simulations

Perform multiple simulation runs by varying the input parameters within their defined ranges. Use *for* loops in MATLAB to automate this process. three *for* loops are used to run simulations multiple times. two *for* loop is for varying the duty ratio D_1 & D_2 of the first converter and second converter, and another *for* loop is for varying the load current of the first converter.

The MATLAB function `simset()` is used to run the SIMULINK file from the MATLAB script environment. For the `simset()` function to access the SIMULINK file, the MATLAB script file and SIMULINK file should be in the same folder.

For each value of the duty ratio and load current range, the simulation file is run, and the output

voltage at that value of duty ratio and load current is recorded.

4.0.2 Data Extraction

Using the **To Workspace** block in the SIMULINK library, load voltage data and load current of both the converter is send to the MATLAB workspace. The load voltage and load current data are stored in the MATLAB workspace, making it simple to access and use for further analysis.

Additionally, the inductor current of both converters 1 and 2 is sent to the MATLAB workspace. This is done to verify whether the first converter is operating in DCM and the second converter is operating in CCM. By examining the inductor current data in MATLAB, we can confirm the operating modes of both converters and ensure that they are functioning as expected during the simulation.

4.0.3 Data Segregation

After each simulation run, the initial data points are removed to eliminate the transient response. The inductor current of the first converter is checked to confirm that at least one value is zero or negative, while the inductor current of the second converter is checked to ensure that all values remain positive. This verifies that the first converter operates in DCM and the second converter operates in CCM.

Once this condition is satisfied, the average values of the load voltage and load current are calculated for both converters. Using the voltage ratios $\frac{V_{in}}{V_{o1}}$ and $\frac{V_{in}}{V_{o2}}$, Sector 1 is identified and the data is grouped accordingly. Then, using Eq. (2.10), if the first converter's load current is greater than $i_{o1(1-9)b}$, it is classified as Sector (1-9) Mode a; otherwise, it is classified as Sector 1 Mode c.

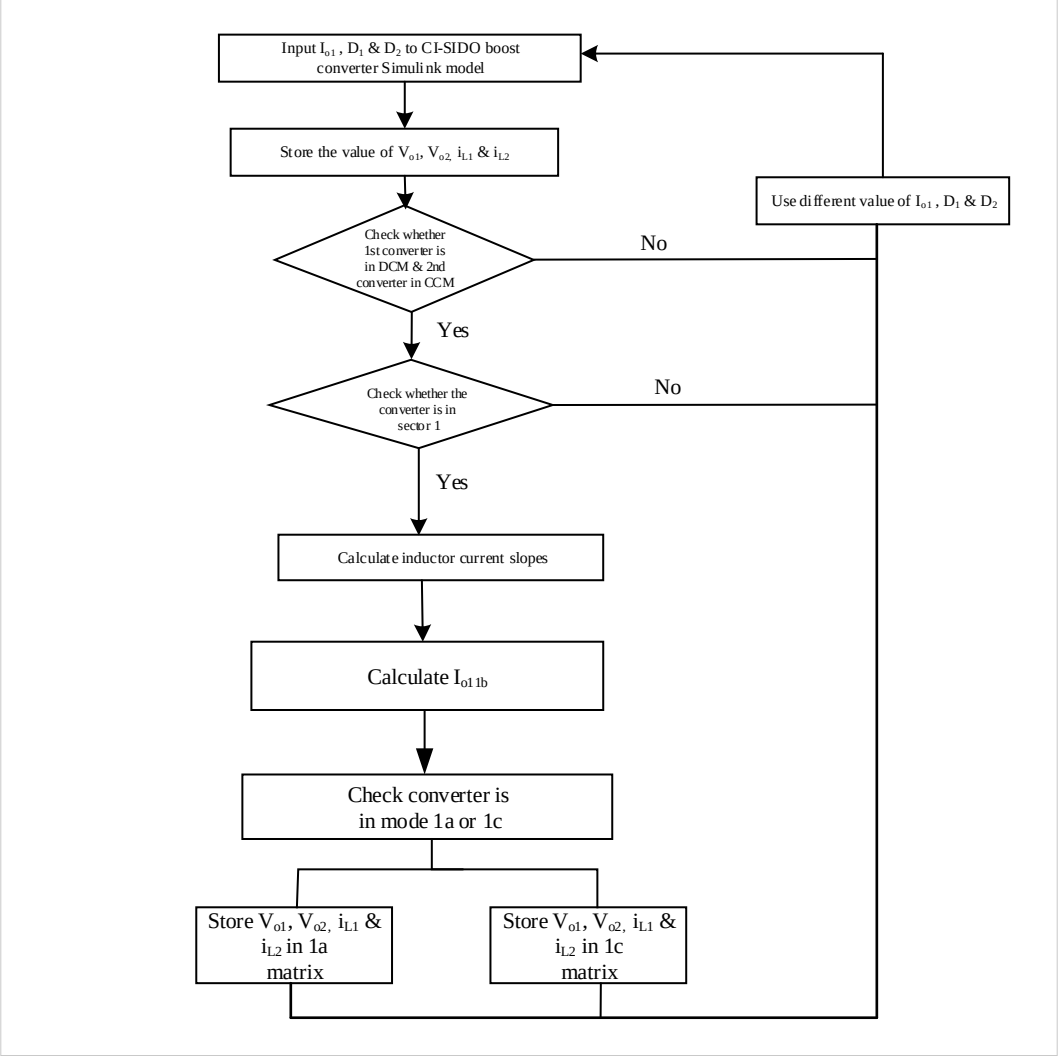

Figure 4.1: Flow chart for collection of data

4.1 Designing the ANN Architecture

The ANN structure is designed based on the required inputs, outputs, and the complexity of the system. The model contains three main parts:

- **Input Layer:** The neural network uses three input variables, the 2-load voltage V_{o1} & V_{o2} and load current I_{o1} of the CI-SIDO converter, so the input layer has 3 neurons.
- **Hidden Layers:** Three hidden layers are used with 32, 16, and 8 neurons. A larger number of neurons is used in the first hidden layer to extract more detailed features from the input data.
- **Output Layer:** Since the Three output of the ANN is the duty ratio D_1 & D_2, and sector

prediction the output layer contains 3 neuron.

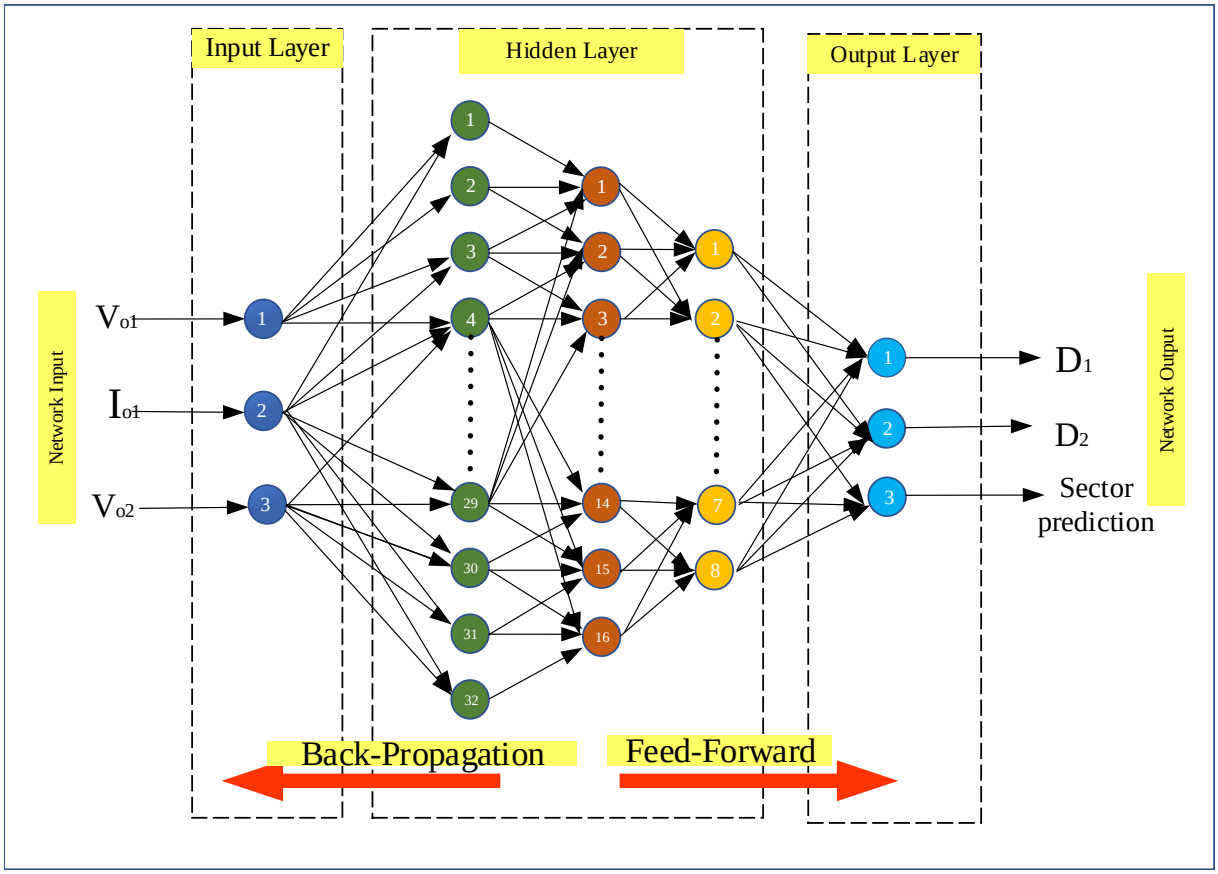

Figure 4.2: Feed-Forward Back-Propagation ANN Architecture

4.2 Training of ANN

After data segregation, the ANN receives the converter's load voltage V_{o1} & V_{o2} and load current as inputs and outputs the duty ratio D_1 & D_2 . The Artificial Neural Network (ANN) model is trained using MATLAB's Neural Network Toolbox (`nntool`). The ANN is trained using the Feed-Forward Back-Propagation algorithm. The tool receives the training parameters, including the number of epochs and learning rates, and uses the data provided to train the neural network.

Table 4.1: Simulation Parameters

Parameters	L_1	L_2	k
Values	48.0 μH	120.0 μH	0.8
Parameters	C_1, C_2	f_s	V_{in}
Values	100 μF	100 kHz	5V

4.3 Implementation as Controller

After training, the ANN is exported to the SIMULINK environment using `gensim()` function. Then, the reference voltage V_{o1} , $V_{o2}$and the actual load current I_{o1} of the converter are given as input to the ANN. Then the ANN will predict the duty ratio D_1 , D_2 And the sector prediction which is given to the CI-SIDO converter as shown in Fig.5.2 ANN only predicts the numerical value, not the alphanumerical value, we are sub-mode a and sub-mode c denoted in 1 and 3 respectively if ANN predict 11 so called sector 1 sub-mode a predict and if it show 13 then its called sector 1 and sub-mode c.

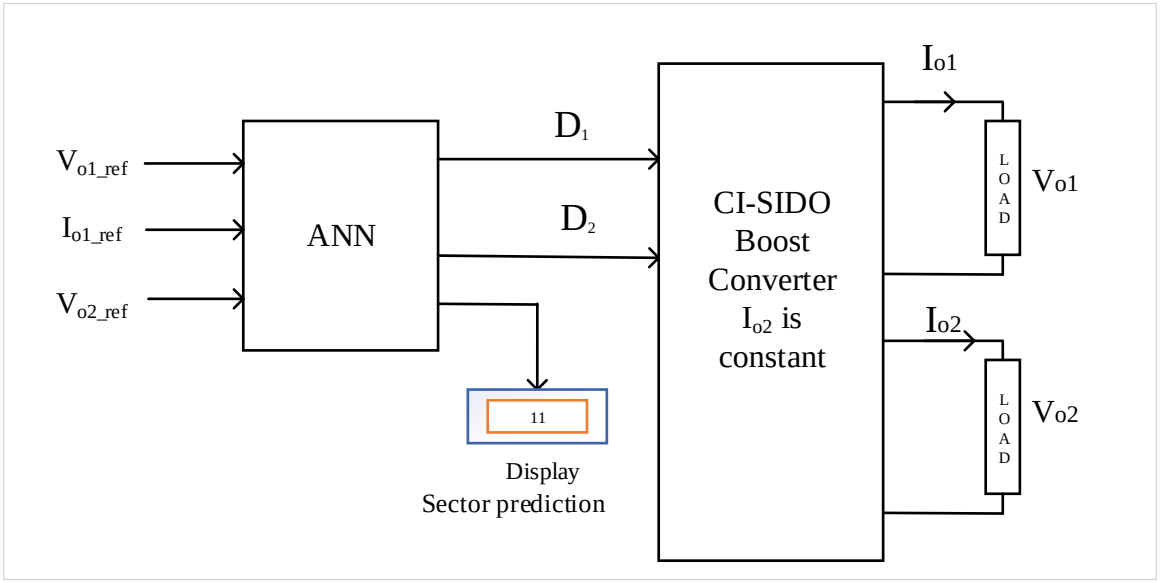

Figure 4.3: ANN as a Controller

4.4 Implementation of ANN using DSP

The hardware implementation of the Artificial Neural Network using a Digital Signal Processor involves developing and training the network in MATLAB/Simulink, extracting the trained parameters, and deploying the model for real-time control. Initially, the ANN is designed and trained in MATLAB using the feedforward backpropagation algorithm, where input–output data from the converter simulation are used to learn the nonlinear relationship between input voltage, inductor current, and the desired output voltage.The trained weights and biases are exported from the MATLAB environment once the neural network achieves the required level of accuracy. The same ANN structure is then replicated on the DSP platform using C programming in Code Composer Studio (CCS) using these values. In order to produce the control signal, the DSP processes input data received through its ADC channels and carries out the feedforward computation of the ANN in real time. The converter's power switches are then operated by PWM pulses generated from this control output. This output is used to generate PWM pulses to drive the power switches of the converter. This approach reduces computational complexity, and demonstrates the practical potential of ANN-based controllers in power electronic systems. The DSP performs real-time feedforward computations of the neural network by processing input data V_{o1},V_{o2} & I_{o1} and generating corresponding control or prediction outputs D_1 and D_2. The generated pulses are then applied to the CI-SIDO converter switches, allowing the converter to achieve the desired output corresponding to the given reference values.

Chapter 5

Simulation Result

5.1 Simulation of CI-SIDO converter

The MATLAB/Simulink model of the CI-SIDO converter is developed and simulated in the MATLAB/SIMULINK environment . The source voltage is assumed to be a ripple-free DC supply with zero source impedance. The inductors are considered ideal with no internal resistance. The capacitors are assumed to be large enough to maintain a ripple-free output voltage. These assumptions help in analyzing the basic performance of the converter under ideal conditions. Following parameters are considered for simulation, $V_{in} = 5$ V, $L_1 = 48\ \mu H$, $L_2 = 120\ \mu H, k = 0.8, C_1 = 100\ \mu F, C_2 = 100\ \mu F, f = 100\ KHz$. For these values $r_{NF1}, r_{NF2}, r_{FN1}$ & r_{FN2} are calculated.

$$r_{NF1} = 0.3360,\ r_{NF2} = 0.4415, r_{FN1} = 0.6640,\ r_{FN2} = 0.5585. \tag{5.1}$$

Using these value duty ratios for all 9 sectors can be obtained. Although it is possible to simulate all nine sectors, the simulation in this carried out in sector 1-9. By choosing $D_1 = 0.01$ to 1 and $D_2 = 0.01$ to 1. The gate pulses (G_1 & G_2), inductor currents (I_{L1}, I_{L2}) and input current (I_{in}) are observed through the scope in the MATLAB/SIMULINK. By observing the Fig. 5.2, we can say $G_{FN1} > 0$ & $GFN2 > 0$ which satisfies the condition for **Sector - 1** in Fig.(2.3a). Similarly, other sectors follow their respective conditions. Hence, by appropriately selecting the duty ratio values, the converter can be operated in different sectors as desired. This has

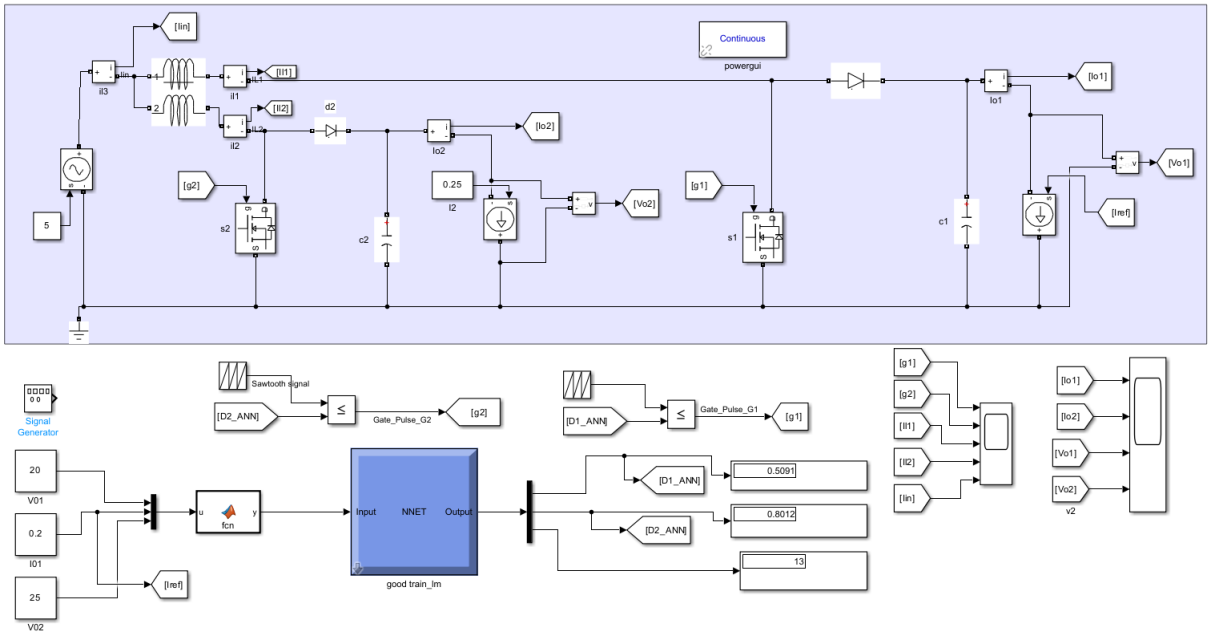

Figure 5.1: Simulink Model of CI-SIDO Converter

been successfully simulated in MATLAB/Simulink.

Table 5.1: Comparison of $D_1(Analytical)$, $D_1(ANN)$, $D_2(Analytical)$, and $D_2(ANN)$

V_{o1} **(V)**	I_{o1} **(A)**	V_{o2} **(V)**	D_1**(Analytical)**	D_1**(ANN)**	D_2**(Analytical)**	D_2**(ANN)**	**Sector**
30	0.2	20	0.6000	0.6054	0.7450	0.7474	1a
20	0.30	30	0.630	0.6318	0.834	0.8324	1a
20	0.1	30	0.4220	0.4312	0.8387	0.8443	1c
6	0.2	25	0.200	0.1952	0.801	0.8216	2c
8	0.25	20	0.1856	0.1947	0.7450	0.7472	2a
6	0.2	25	0.0195	0.0200	0.8200	0.8216	3
20	0.2	12	0.4200	0.4092	0.5850	0.5823	4a
8	0.4	12	0.2100	0.1952	0.5850	0.586	5a
8	0.06	12	0.0610	0.0545	0.5950	0.6003	5c
15	0.2	8	0.418	0.4126	0.3520	0.3452	7a
8	0.2	5	0.2856	0.2850	0.0522	0.0600	8a
5	0.1	5	0.0554	0.066	0.0350	0.0385	9

From Table 5.1, it is observed that the duty cycles obtained using the ANN model (D_1(ANN) and D_2(ANN)) closely match the analytical values (D_1(Analytical) and D_2(Analytical)) for all operating conditions. The slight deviations are minimal, indicating that the ANN model accurately learns the nonlinear relationship between input and output variables of the converter. Hence, the ANN-based approach can effectively predict the required duty cycles with high precision and reliability.

The results of the simulation are shown on the following next pages. The ANN predicts the corresponding duty ratios D_1 and D_2 using reference values for V_{o1}, I_{o1} and V_{o2}. The reference voltage and current values are nearly met by the simulated values.

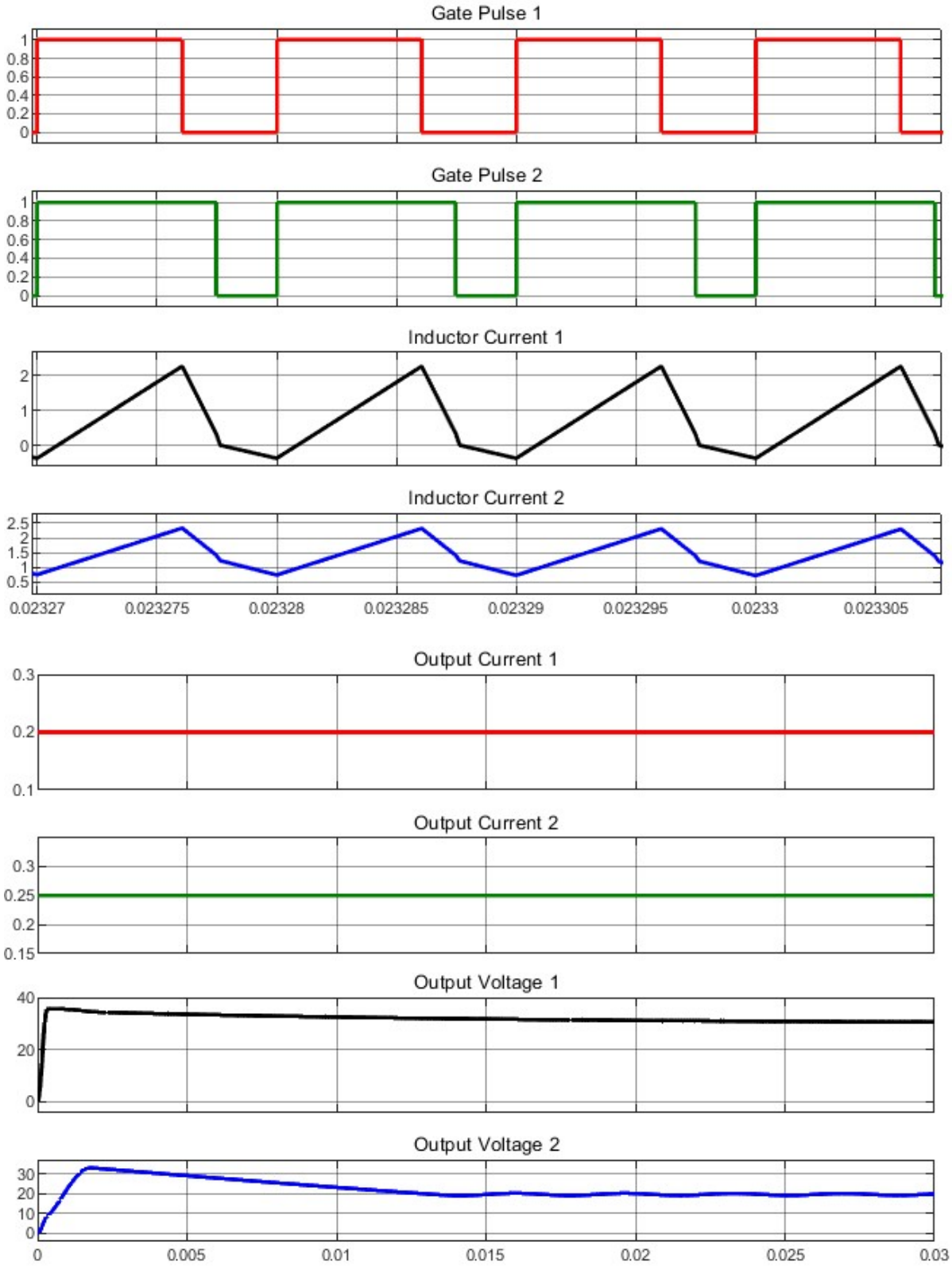

Figure 5.2: Simulation of CI-SIDO Boost Converter Sector- 1, sub-mode-a
Ref. Voltage & current of ANN V_{o1} =30V, V_{o2} = 20V & I_{o1}=0.2Amp

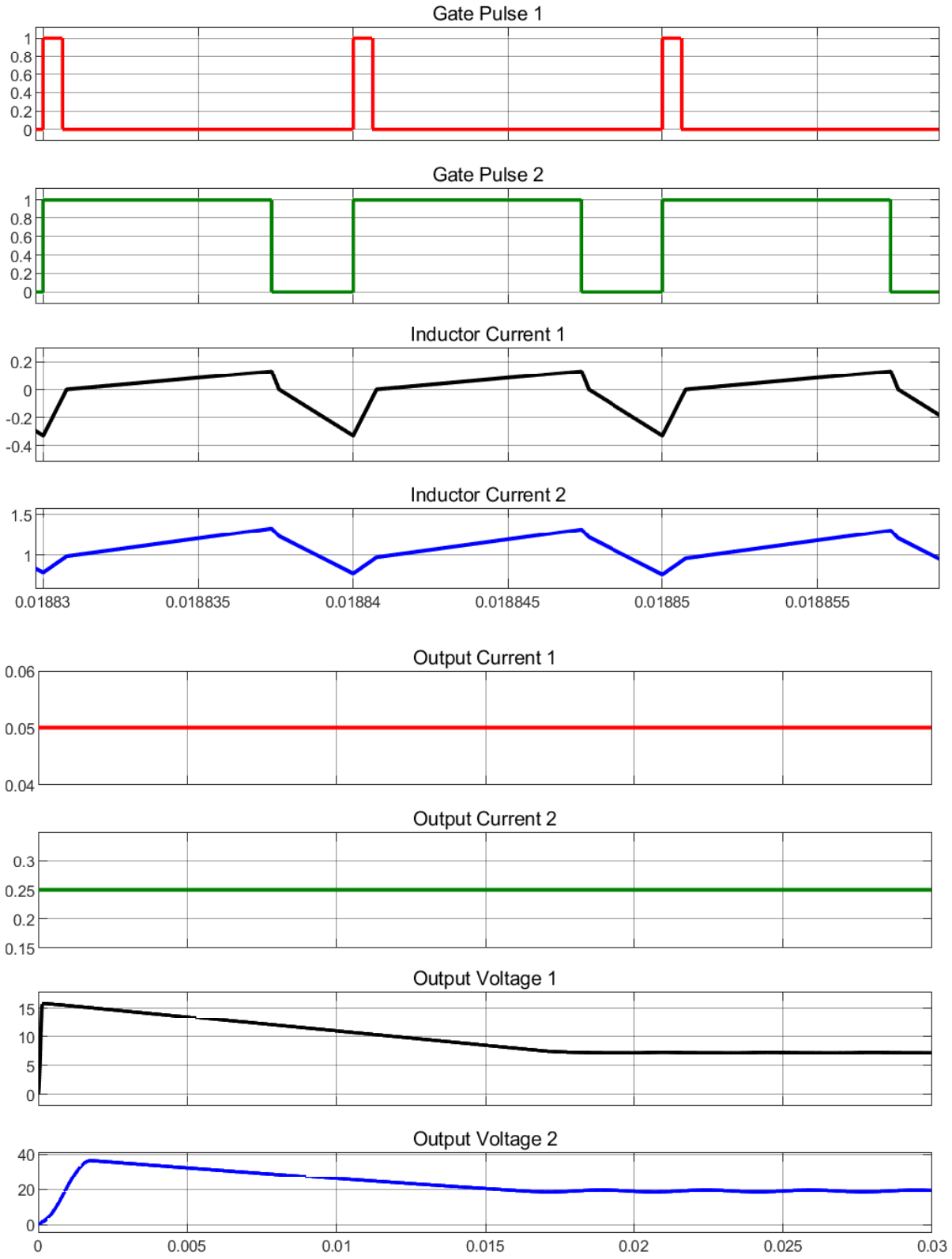

Figure 5.3: Simulation of CI-SIDO Boost Converter Sector- 2, sub-mode a,
Ref. Voltage & current of ANN V_{o1} =8V, V_{o2} =20V & I_{o1} =0.05Amp

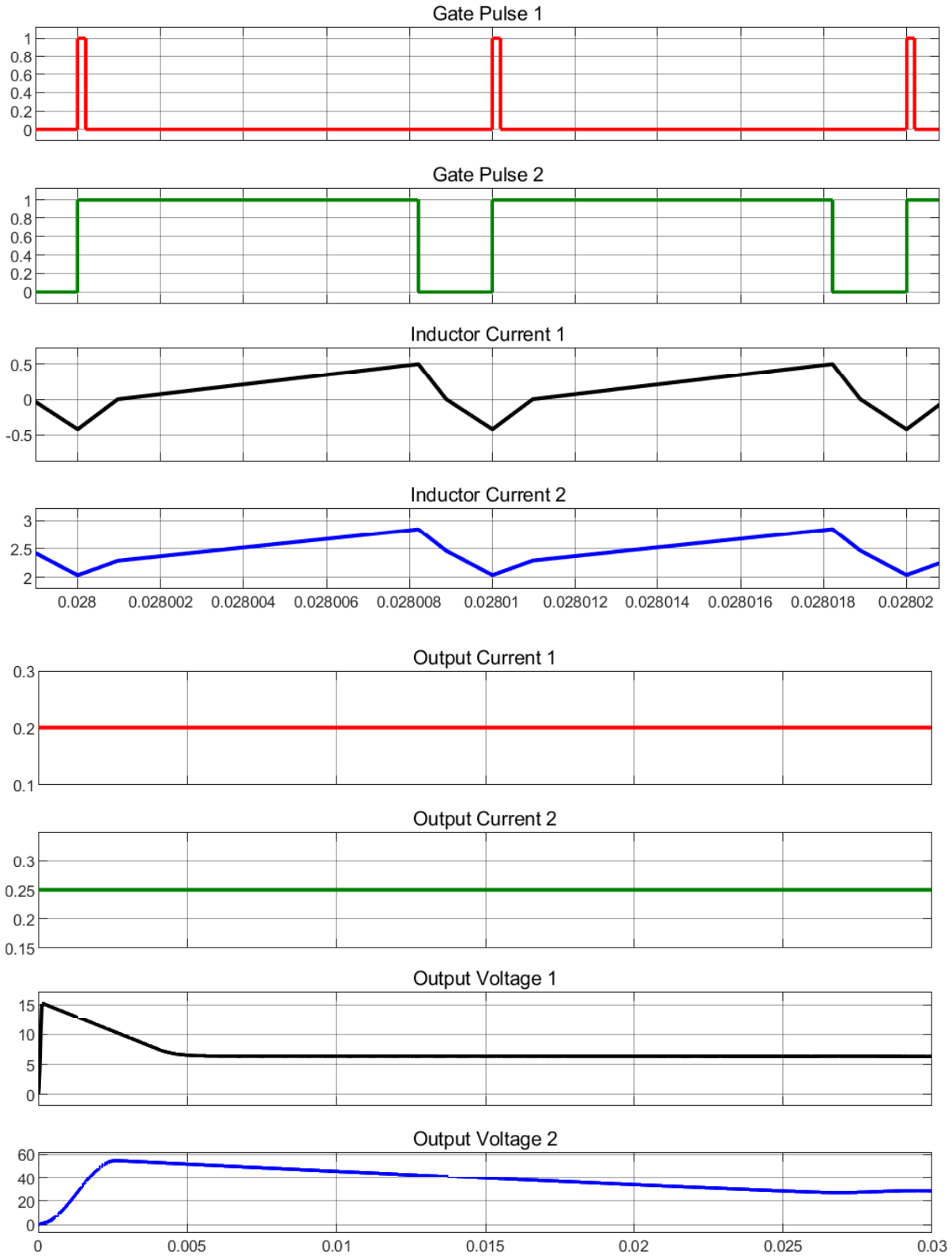

Figure 5.4: Simulation of CI-SIDO Boost Converter Sector- 3,
Ref. Voltage & current of ANN V_{o1} =6V, V_{o2} =25V & I_{o1} =0.2Amp

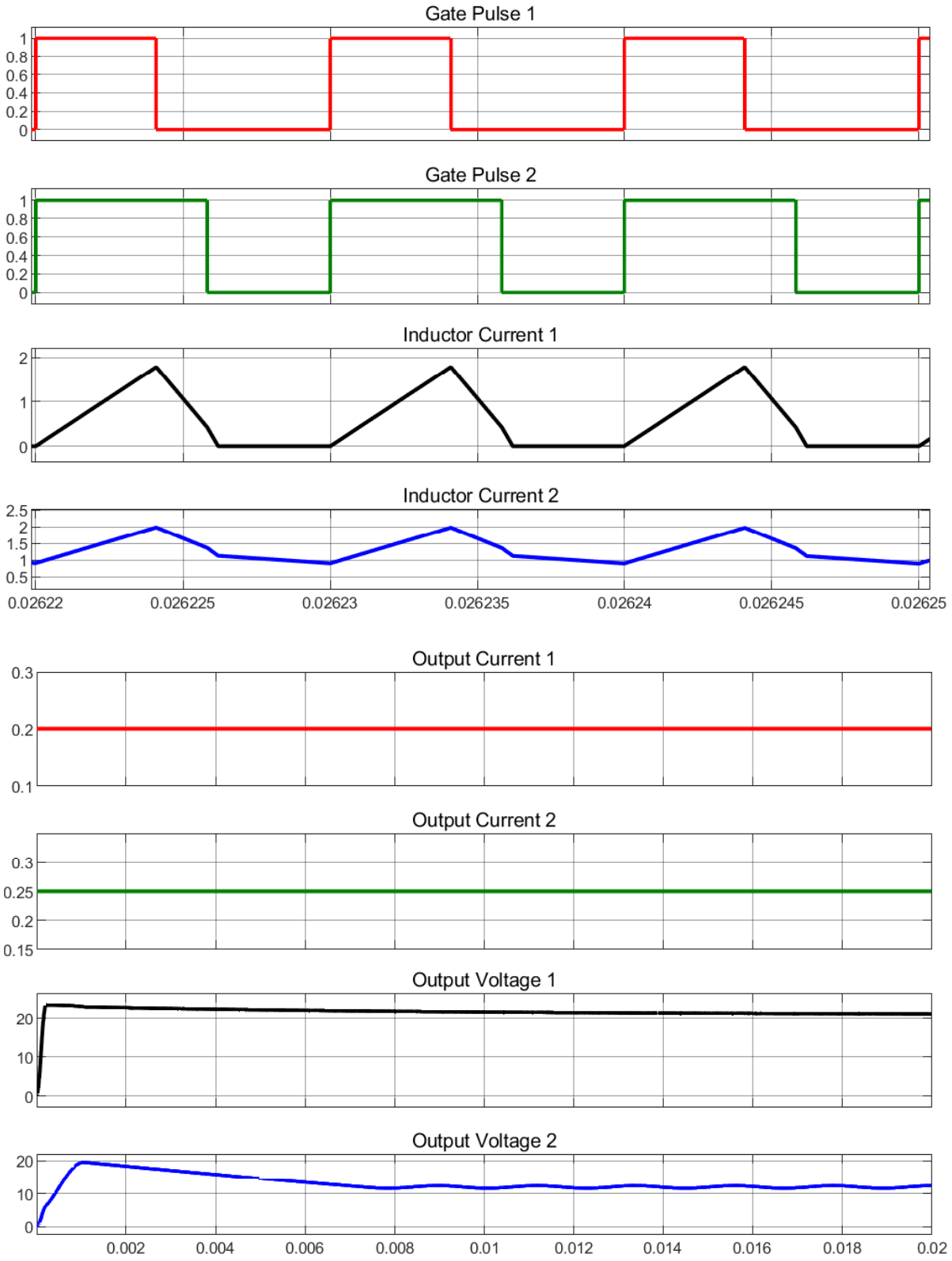

Figure 5.5: Simulation of CI-SIDO Boost Converter Sector- 4a,
Ref. Voltage & current of ANN V_{o1} =20V, V_{o2} =12V & I_{o1} =0.2Amp

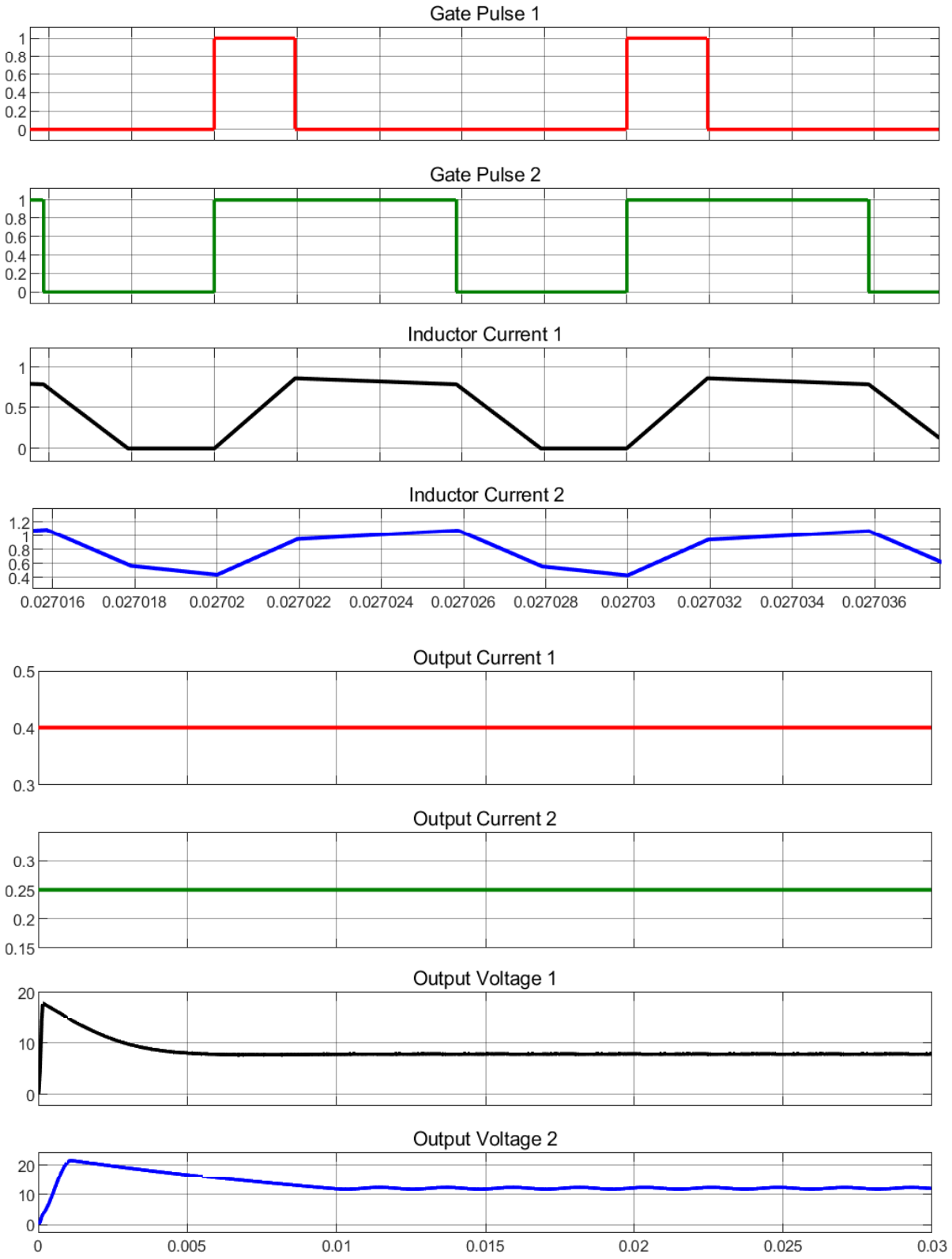

Figure 5.6: Simulation of CI-SIDO Boost Converter Sector- 5a,
Ref. Voltage & current of ANN V_{o1} =8V, V_{o2} =12V & I_{o1} =0.4Amp

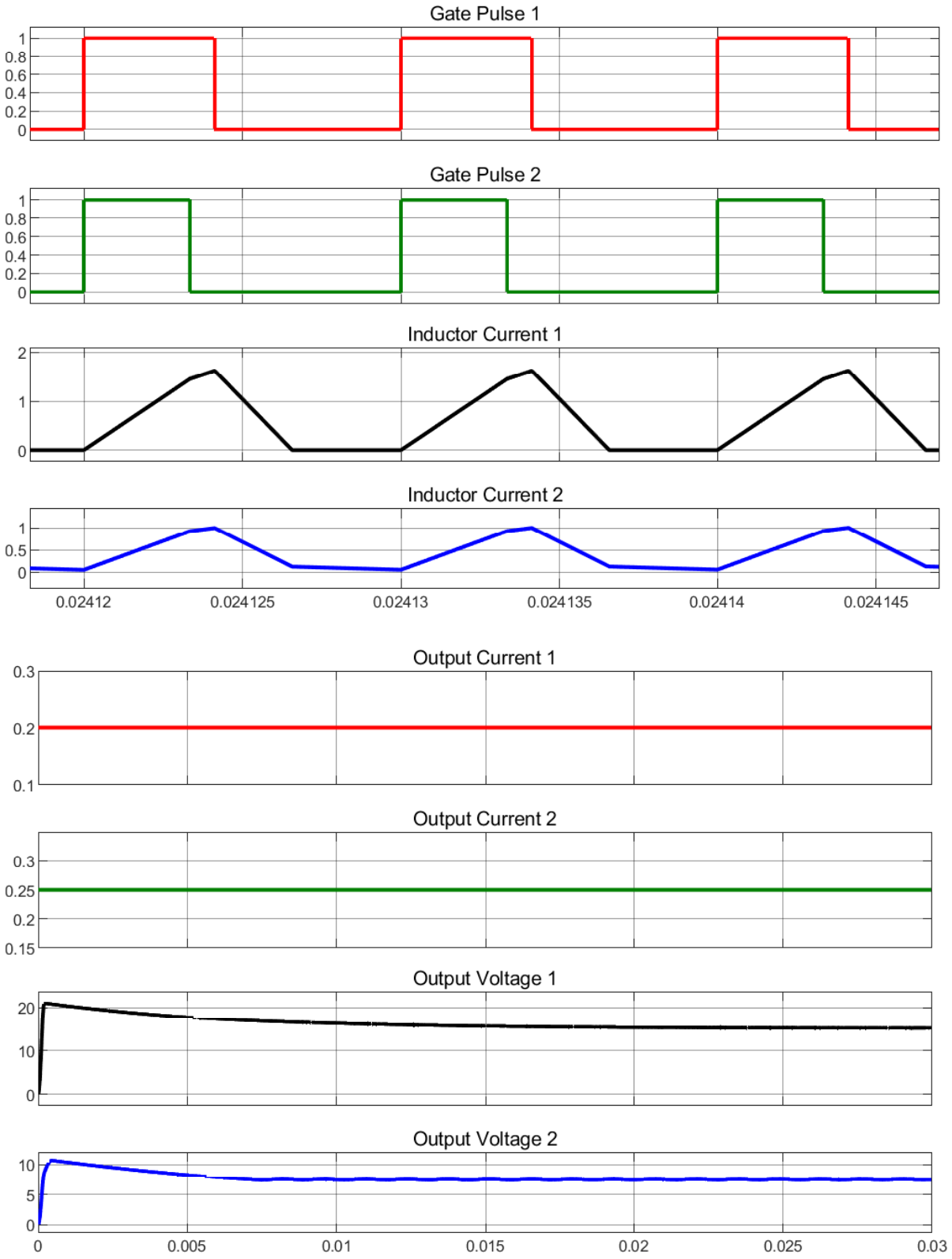

Figure 5.7: Simulation of CI-SIDO Boost Converter Sector- 7 and Sub-mode a, Ref. Voltage & current of ANN V_{o1} =15V, V_{o2} =8V & I_{o1} =0.2Amp

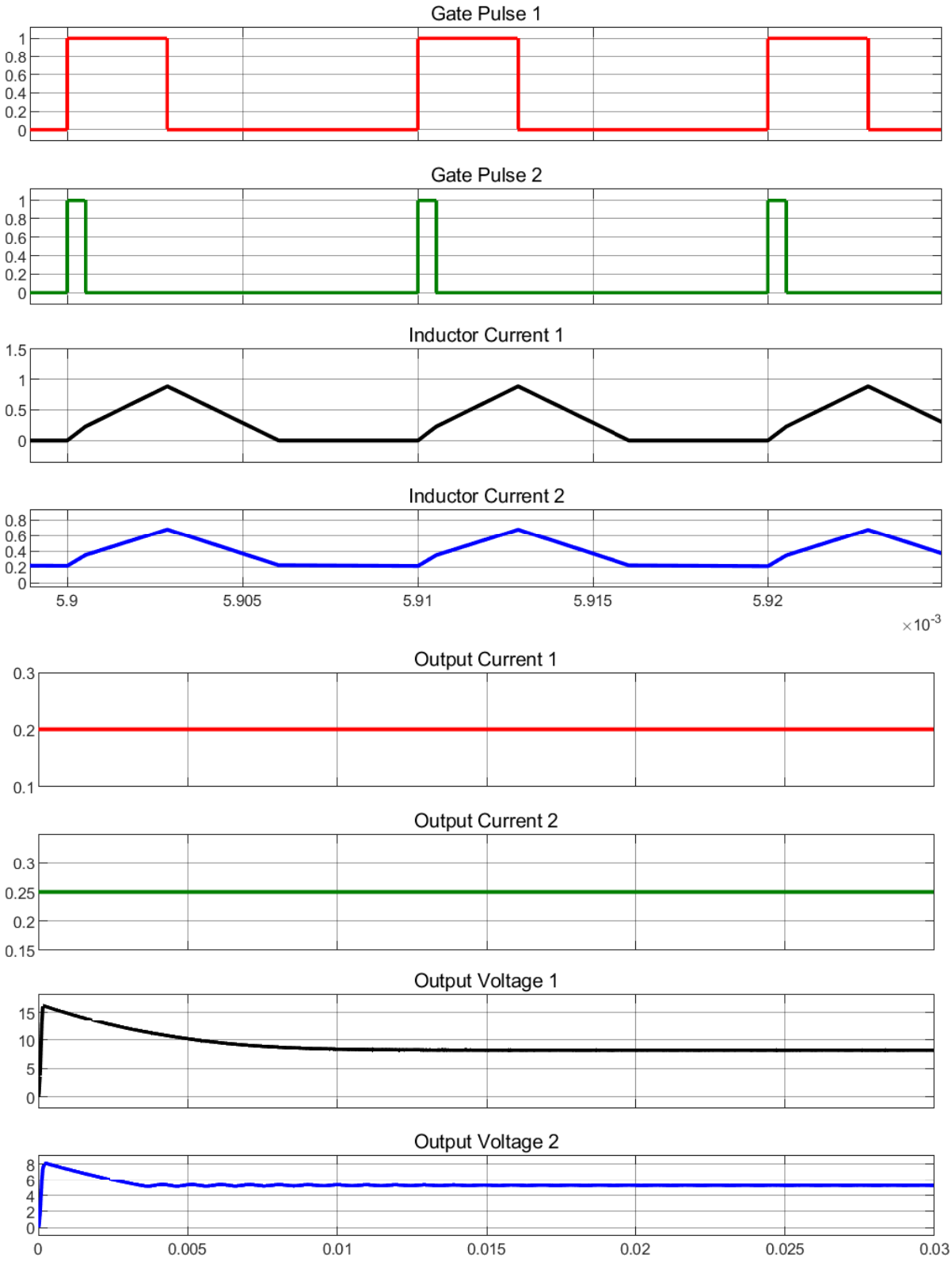

Figure 5.8: Simulation of CI-SIDO Boost Converter Sector- 8 and Sub-mode a, Ref. Voltage & current of ANN V_{o1} =8V, V_{o2} =5V & I_{o1} =0.2Amp

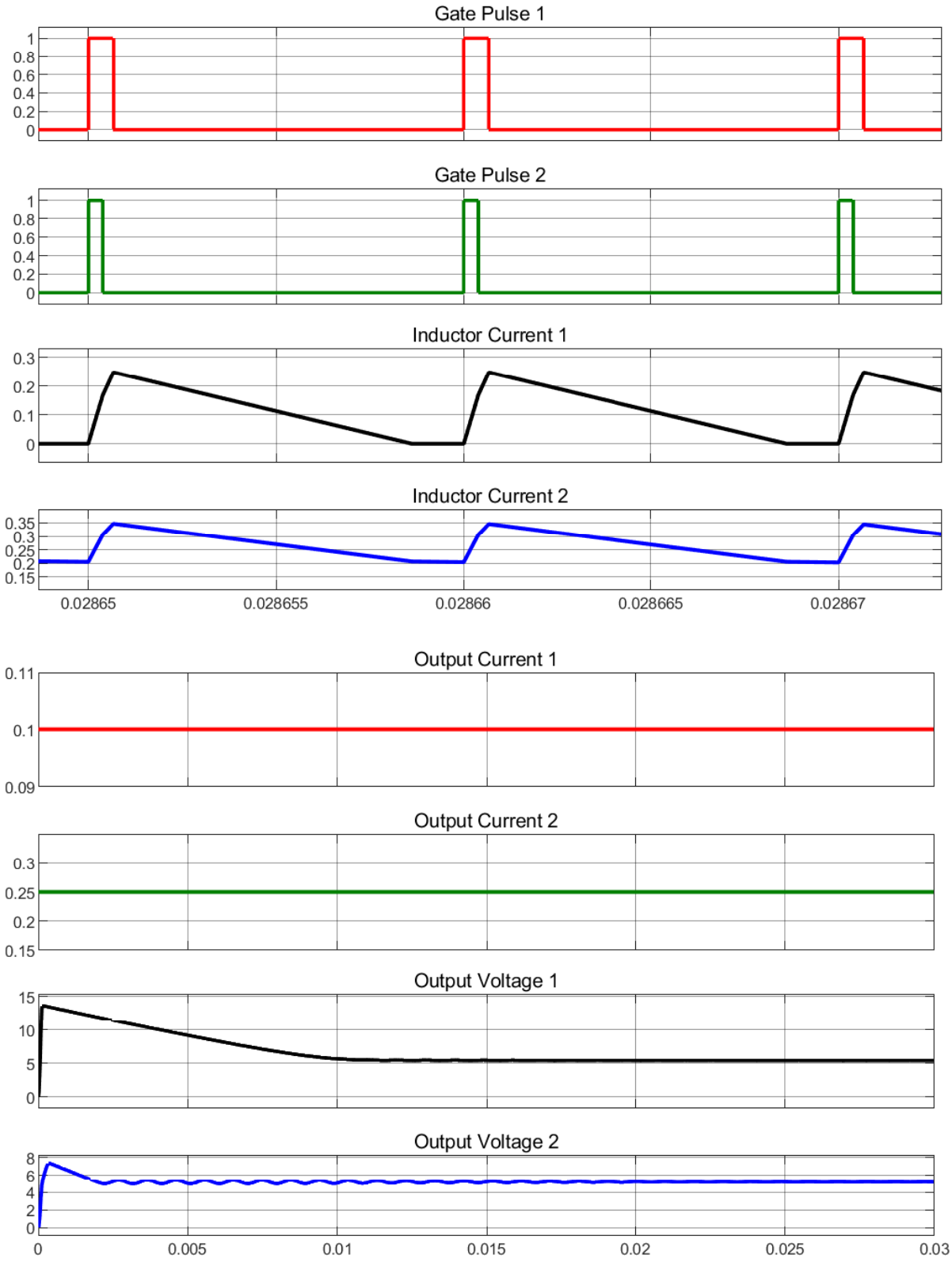

Figure 5.9: Simulation of CI-SIDO Boost Converter Sector- 9,
Ref. Voltage & current of ANN V_{o1} =5V, V_{o2} =5V & I_{o1} =0.1A

5.2 PWM Pulse Generation Using DSP

The Artificial Neural Network (ANN) is first trained in Sector 1 and sector 4 using simulation data obtained from MATLAB/Simulink. The ANN learns the relationship between the input parameters (V_{o1}, V_{o2}, and I_{o1}) and the desired duty ratios (D_1 and D_2) during the training process. The optimised weights and biases are taken out of the MATLAB model after the ANN has been trained. The ANN is then implemented in real time by programming these trained parameters into the DSP (Digital Signal Processor). The DSP predicts the necessary duty ratios D_1 and D_2 by reading the actual converter outputs as inputs to the ANN model. The DSP creates matching PWM pulses to regulate the converters based on these anticipated values. This procedure enables the system to achieve stable operation under a range of load conditions and automatically control the output voltage.

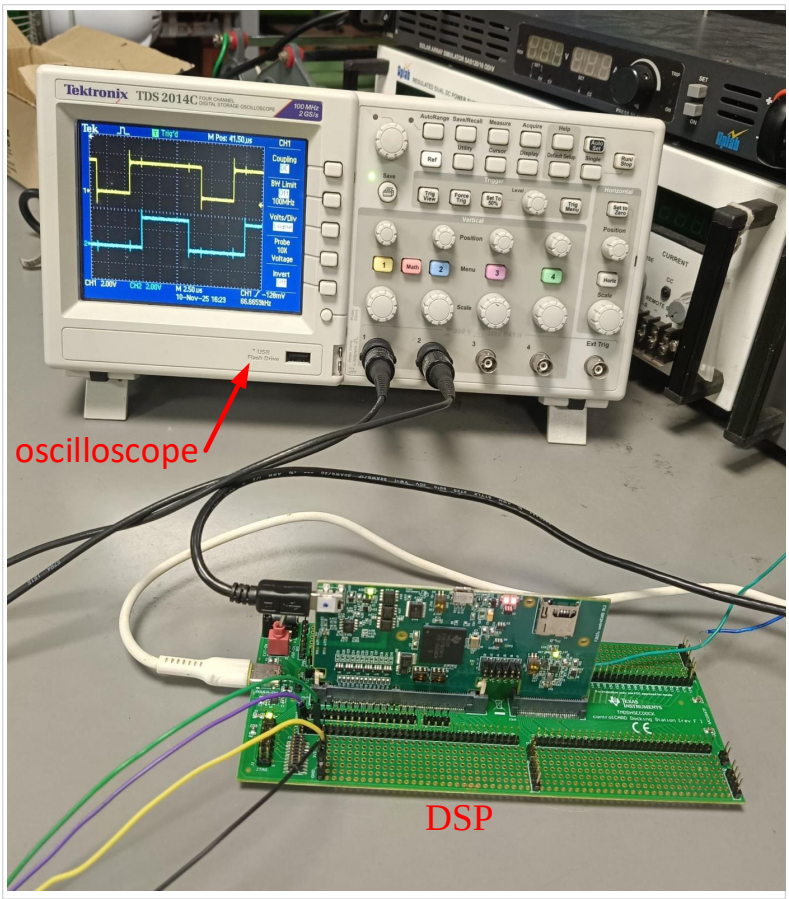

Figure 5.10: Hardware setup.

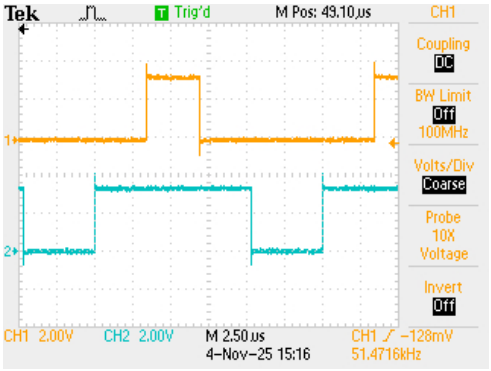

(a) Mode 1c

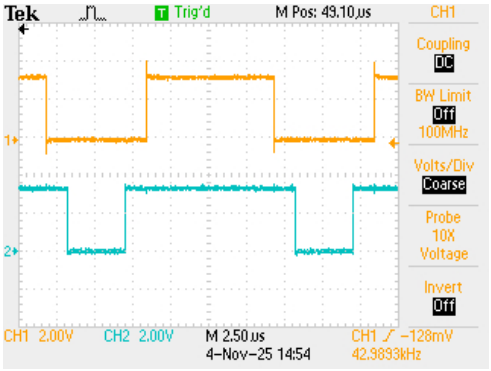

(b) Mode 1a

Figure 5.11: Waveforms of g_1 and g_2 during operation in Mode 1c and Mode 1a of the CI-SIDO boost converter.

for figure-5.10a, the given reference values of $V_{o1} = 15\,\text{V}$, $I_{o1} = 0.1\,\text{A}$, and $V_{o2} = 15\,\text{V}$, the trained ANN predicts the corresponding duty ratios as $D_1 = 0.2375$ and $D_2 = 0.6876$.

for figure-5.10b, the given reference values of $V_{o1} = 20\,\text{V}$, $I_{o1} = 0.3\,\text{A}$, and $V_{o2} = 20\,\text{V}$, the trained ANN predicts the corresponding duty ratios as $D_1 = 0.5575$ and $D_2 = 0.7505$.

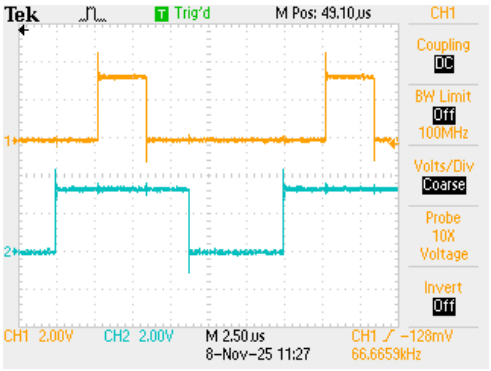

(a) Mode 4c

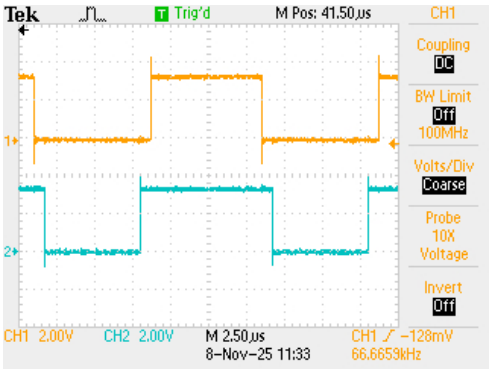

(b) Mode 4a

Figure 5.12: Waveforms of g_1 and g_2 during operation in Mode 4c and Mode 4a of the CI-SIDO boost converter.

for figure-5.11a, the given reference values of $V_{o1} = 15\,\text{V}$, $I_{o1} = 0.1\,\text{A}$, and $V_{o2} = 12\,\text{V}$, the trained ANN predicts the corresponding duty ratios as $D_1 = 0.2121$ and $D_2 = 0.5858$.

for figure-5.11b, the given reference values of $V_{o1} = 25\,\text{V}$, $I_{o1} = 0.2\,\text{A}$, and $V_{o2} = 12\,\text{V}$, the trained ANN predicts the corresponding duty ratios as $D_1 = 0.4899$ and $D_2 = 0.5814$.

Conclusion

Determining the duty ratio of the CI-SIDO boost converter operating in DCM is complex. to simplify this process using an ANN model to determine the duty ratios D_1 and D_2, as well as to identify the operating sector and mode of the converter. In this system, the first converter operates in Discontinuous Conduction Mode, while the second converter functions in Continuous Conduction Mode. The accuracy of the ANN model is verified through analytical calculations and MATLAB/Simulink simulations of the CI-SIDO boost converter. after that we are implementing an Artificial Neural Network (ANN) using a Digital Signal Processor (DSP) that successfully demonstrates the intelligent control of the CI-SIDO boost converter. By accurately predicting the duty ratios D_1 and D_2 for various converter operating modes, such as DCM and CCM, the ANN lessens the need for intricate analytical models. which guaranties faster computation and precise pulse generation. All things considered, the combination of ANN and DSP provides a strong option for high-speed, open loop control in power electronics applications.

Bibliography

[1] D. M. Bellur and M. Kazimierczuk., "DC-DC converters for ev applications," in *2007 Electrical Insulation Conference and Electrical Manufacturing Expo*. IEEE, 2007, pp. 286–293.

[2] M.-C. Lee., JB. Lio, D. Y. Chen, and Y.-P. Wu, "Small-signal modeling of multiple-output flyback converters in CCM mode with weighted feedback," *IEEE Transactions on Industrial Electronics*, vol. 45, no.- 2, pp. 236–248, 1998.

[3] Q. Chen, F.C.-Lee, and M.j. Jovanovic, "Analysis and design of weighted voltage-mode control for a multiple-output forward converter," in *Proceedings Eighth Annual Applied Power Electronics Conference and Exposition,*. IEEE, 1993, pp. 449–455.

[4] N.-S. Pham, T.M. Yoo., T.-H. Kim, C.-G. Lee, and K.-H. Baek, "A 0.016 mv/ma cross-regulation 5-output simo dc–dc buck converter using output-voltage-aware charge control scheme," *IEEE Transactions on Power Electronics*, vol. 33, no. 11, pp. 9619–9630, 2017.

[5] A. -Ikriannikov and T. Schmid, "Magnetically coupled buck converters," in *2013 IEEE Energy Conversion Congress and Exposition*. IEEE, 2013, pp. 4948–4954.

[6] W. Xu, X. Gong, Z. Hong, and D. Killat, "A dual-mode single-inductor dual-output switching converter with small ripple," *IEEE Trans. Power Electron.*, vol. 25, pp. 614–623, Mar. 2010.

[7] Y. Wang, J. Xu, and G. Yin, "Cross-regulation suppression and stability analysis of capacitor current ripple controlled SIDO ccm buck converter," *IEEE Transactions on Industrial Electronics*, vol. 66, no. 3, pp. 1770–1780, 2018.

[8] J. D.- Dasika, B. Bahrani, M. Saeedifard, and A. Rufer,"Multivariable control of single-inductor dual-output buck converters," *IEEE Transactions on Power Electronics*, vol. 29, no. 4, pp. 2061–2070, 2013.

[9] M.-Y. Jung, S.-u. Shin, and G.-H. Chho, "Issues of single-inductor multiple-output dc-dc converters," in *2015 International SoC Design Conference (ISOCC)*. IEEE, 2015, pp. 115–116.

[10] G. Chen, Y. Deng, J. Dong, Y. Hu, L. Jiang, and X. He, "Integrated multiple-output synchronous buck converter for electric vehicle power supply," *IEEE Transactions on Vehicular Technology*, 2016.

[11] Nupur, "Ripple minimization of input and inductor currents in coupled inductor single input dual output dc-dc converters," phd-thesis, Department of Electronics and Electrical Engineering, IIT Guwahati, Jan. 2023.

[12] S. Nath *et al.*, "Effect of coupling on discontinuous conduction mode of coupled inductor sido boost converter," *IEEE Transactions on Power Electronics*, vol. 37, no. 5, pp., 2021.

[13] D. S. Chintu, S. Nath *et al.*, "Effect of coupling on input-output voltage relations in DCM of sido boost converters," in *2021 National Power Electronics Conference (NPEC)*. IEEE, 2021.

[14] F. Kurokawa, A. Yamanishi, and S. Hirotaki, "A reference modification model digitally controlled dc-dc converter for improvement of transient response," *IEEE Transactions on Power Electronics*, vol. 31, pp. 871–883, 2015.

[15] J. Liue, T.A. Wei, N. Chen, J. Wu., P. Xiao, and Y. Luo, "A backpropagation neural network controller trained using PID for digitally-controlled dc-dc switching converters," in *2021 IEEE 16th Conference on Industrial Electronics and Applications (ICIEA)*. IEEE, 2021, pp. 946–951.